PCCP

PAPER

View Article Online
View Journal | View Issue

Open Access Article. Published on 27 June 2022. Downloaded on 10/30/2025 7:29:39 PM.
This article is licensed under a Creative Commons Attribution-NonCommercial 3.0 Unported Licence.

Check for updates

Cite this: *Phys. Chem. Chem. Phys.*, 2022, **24**, 16755

New insights into the interaction of triethylphosphine oxide with silica surface: exchange between different surface species†

Elisabet Pires and José M. Fraile*

Received 7th April 2022,
Accepted 27th June 2022

DOI: 10.1039/d2cp01621d

rsc.li/pccp

Although chemical shift values of triethylphosphine oxide (TEPO) adsorbed on acidic solids have been considered as an indication of acid strength, in this work we demonstrate that the chemical shift depends also on the adsorbed amount of TEPO. On silica, the presence of three different adsorbed species, physisorbed on non-acidic surface, chemisorbed through a single H bond and chemisorbed through two H bonds, can be detected by the correlation of the ^{31}P chemical shift with the TEPO adsorbed amount. TEPO chemical exchange between the different sites is demonstrated by the single NMR signal obtained in all the cases, and also by the variation of the line width, which is broader at low surface coverage due to the slower chemical exchange because of the longer average distance between surface sites.

Introduction

Trialkylphosphine oxides have been recognized as useful probes for the characterization of the acidity of solid catalysts by ^{31}P solid state NMR.[1,2] Triethylphosphine oxide (TEPO) was initially used,[3] in analogy with the method for the determination of acceptor number (AN) of solvents.[4] Later on, other trialkylphosphine oxides, such as trimethylphosphine oxide (TMPO) or tributylphosphine oxide (TBPO), have been also employed, in order to get information not only about acid strength, but also about the acid type (Brønsted or Lewis), the location and the amount of the acid sites.[2] The ^{31}P chemical shift (δ) of the adsorbed trialkylphosphine oxides has been used as an indicator of the strength of the Brønsted acid sites,[5] and they have been even predicted by DFT calculations in the case of zeolites.[6,7]

In the most commonly used method for determination of δ, samples are prepared by adsorption of TEPO from a solution in a non-polar solvent, usually anhydrous pentane[5,8–12] or hexane.[5] However, the adsorbed amount of TEPO varies in the different published works. The used TEPO/solid ratios include 0.74 mmol g^{-1} (9.9 wt%),[5] 10 wt%,[8,12] 15 wt%,[9,11] and 20 wt%.[10] Given the variability in the functionalization of the different solids, the TEPO/acid ratio was even different from one catalyst to another in each work. For example, in the case of materials functionalized with sulfonic acids, the ranges of TEPO/sulfonic sites molar ratios were 0.33–1.96 for SBA15–SO_3H,[8] 0.40–11.18 for carbon–silica composites,[9] 1.34–5.96 for mesoporous periodic organosilicas,[10] or 1.04–7.99 for sulfonated graphene oxide and other carbon materials.[11] As can be seen, the TEPO amount ranged from below the stoichiometric amount to far over stoichiometric ones. In all the cases, the changes in ^{31}P chemical shift were interpreted as differences in the acid strength of the sulfonic sites, irrespective from this TEPO/acid sites ratio.

In solution, we have recently described the determination of the ^{31}P δ for the acid–TEPO 1:1 species, which is significantly different from the values used for AN calculation, as they are measured at infinite dilution, that is extrapolating to zero TEPO/acid molar ratio. The variation in acid/TEPO molar ratio in solution produces a variation in ^{31}P chemical shift due to the contribution of different species, namely free TEPO, acid–TEPO 1:1 and even acid–TEPO 2:1, in rapid exchange.[13] In the case of solids with highly dispersed single acid sites on the surface, the adsorption of an excess of TEPO over the acid sites (TEPO/acid molar ratio $>$ 1) should produce at least two NMR signals, corresponding to TEPO-acid species and physisorbed TEPO on the non-acidic solid surface. In the case of solids without a fully controlled structure, such as carbon based materials, several signals were obtained with a difficult interpretation.[9–12,14] On the contrary, on solids with a regular structure, such as sulfonated polystyrene, one single signal was obtained, which was assigned to the sulfonic–TEPO 1:1 species.[15]

Silica is a weakly acidic solid which has been also extensively used as support for strong acid sites. In principle, the only acid sites present on silica are silanol groups (Si–OH) that should

Instituto de Síntesis Química y Catálisis Homogénea, CSIC-Universidad de Zaragoza, Facultad de Ciencias, Pedro Cerbuna 12, E-50009 Zaragoza, Spain. E-mail: jmfraile@unizar.es, josem.fraile@csic.es

† Electronic supplementary information (ESI) available: ^{31}P MAS NMR spectra of TEPO adsorbed on all the silica materials at the different loadings; comparison of behavior of TEPO ^{31}P chemical shift with surface coverage on solid state NMR spectra and with TEPO/acetic acid in the solution spectra; pore size distribution of solids. See DOI: https://doi.org/10.1039/d2cp01621d

Open Access Article. Published on 27 June 2022. Downloaded on 10/30/2025 7:29:39 PM.
This article is licensed under a Creative Commons Attribution-NonCommercial 3.0 Unported Licence.

produce a single NMR signal of adsorbed TEPO. In previous papers, the ^{31}P chemical shift of TEPO adsorbed on silica has been reported at 56 ppm[5] and 62.3 ppm[15] on silica gel, and 58.5 ppm on periodic mesoporous organosilica.[10] This quite important variation in chemical shift, more than 6 ppm (analogous to the variation from acetic to trifluoroacetic acid in solution[13]), can hardly be ascribed to variations in the acid strength of the silanol groups. In this paper we describe the variation in ^{31}P δ with the amount of adsorbed TEPO on different silicas, together with an interpretation of these differences based on the possible TEPO–silanol interactions.

Experimental

Materials

Aerosil 200 (non-porous pyrogenic silica) was purchased from Degussa. MCM-41 (mesoporous crystalline silica) was purchased from Merck. Silia P60 (porous precipitated silica) was purchased from Silicycle. Pretreatment of silicas at 200 °C or 500 °C were carried out under dry air flow in a tubular furnace with a temperature ramp of 1 °C min^{-1}, followed by a plateau of 4 h at the desired temperature. The hot samples (120 °C) were quickly transfer to a close glove box and since then they were handled under Ar atmosphere. Surface area and pore volume were determined from the N_2 adsorption–desorption isotherms by the BET method in a Micromeritics ASAP 2020 apparatus. The values are gathered in Table 1.

NMR experiments

To each sample of pretreated silica (30 mg), the volume of TEPO solution in anhydrous hexane (15 mM) required for the desired TEPO loading was added. The mixture was stirred for 24 h and then the solvent was evaporated under reduced pressure.

Solid state NMR spectra were recorded in a Bruker Avance III WB400 spectrometer with 4 mm zirconia rotors spun at magic angle in N_2 at 10 kHz. ^{31}P NMR spectra (150 to 2000 scans) were recorded at 162 MHz using a ^{31}P $\pi/2$ pulse length of 4.3 μs and 30 s recycle delay. Pulses and chemical shifts were calibrated with $(NH_4)H_2PO_4$.

Table 1 Silicas used in this work

Silica	Pretreatment temperature (°C)	Surface area (m^2 g^{-1})	Pore volume[a] (cm^3 g^{-1})	Porediameter[a] (nm)
Aerosil	200	207	—	—
200	500	199	—	—
MCM-	200	979	0.85	2.85
41	500	991	0.88	2.96
Silia	200	423	0.84	5.78
P60	500	463	0.79	5.20

[a] BJH desorption value.

Results and discussion

The study of a large number of silicas pretreated at different temperatures by different techniques, such as thermogravimetry and deuterium exchange gave rise to the. Zhuravlev model.[16] In this model, the silanol surface density can be considered as a physico-chemical constant, which is only a function of the pretreatment temperature and it is not dependent on the origin and textural properties of the silica. Taking this model into account, there are three types of silanol groups on the external surface of silica, namely isolated, geminal and vicinal (Fig. 1), together with hydrophobic siloxane (Si–O–Si) bonds. The vicinal silanols can be eliminated by calcination at 400 °C or higher, leading to a more uniform surface.

TEPO adsorption on Aerosil 200

Aerosil 200 is a non-porous pyrogenic silica whose surface properties have been deeply studied by different methods, such as FTIR,[17–19] or MAS ^{1}H NMR.[20,21] Hence it was initially chosen as the simplest case to study the TEPO adsorption. Aerosil 200 was calcined at 500 °C in order to control the amount of acidic silanol groups, leaving only isolated and geminal ones.[16,20] The weight loading of TEPO on silica was systematically varied from 1 to 30 wt%. The ^{31}P solid state MAS-NMR spectra were registered using a single-pulse sequence at 10 kHz spinning speed, as experiments with ^{1}H–^{31}P high power decoupling and cross-polarization did not show any advantage and identical spectra were obtained. As can be seen in Fig. 2, two interesting features can be observed when comparing the ^{31}P NMR spectra at different TEPO loading: first, a single signal was obtained regardless the TEPO weight loading, secondly the signal showed an increasing linewidth when decreasing the TEPO loading. This behaviour is completely different from the effect of TMPO loading in the case of H-ZSM-5 zeolite, where a large number of signals were obtained in the range of 60–200 wt% loading.[22]

The presence of a single signal of variable chemical shift (from 61.2 to 51.5 ppm for TEPO loading from 1 to 30 wt%) seems to indicate the existence of a fast equilibrium between different species on the surface, and it cannot be ascribed to differences in acid strength. This observation leads to a first important conclusion: a single result of ^{31}P chemical shift should not be taken as indication of the acid strength of the site on the solid surface, as variations in δ can be produced by other causes.

Variable temperature experiments were performed in an attempt to slow down the exchange, allowing the detection of

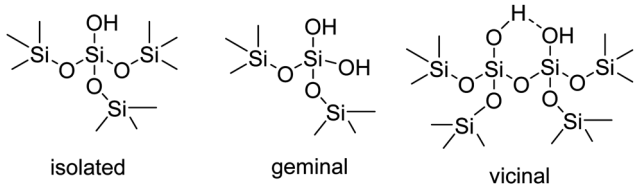

Fig. 1 General types of silanol groups on the external surface of silica.

Open Access Article. Published on 27 June 2022. Downloaded on 10/30/2025 7:29:39 PM.
This article is licensed under a Creative Commons Attribution-NonCommercial 3.0 Unported Licence.

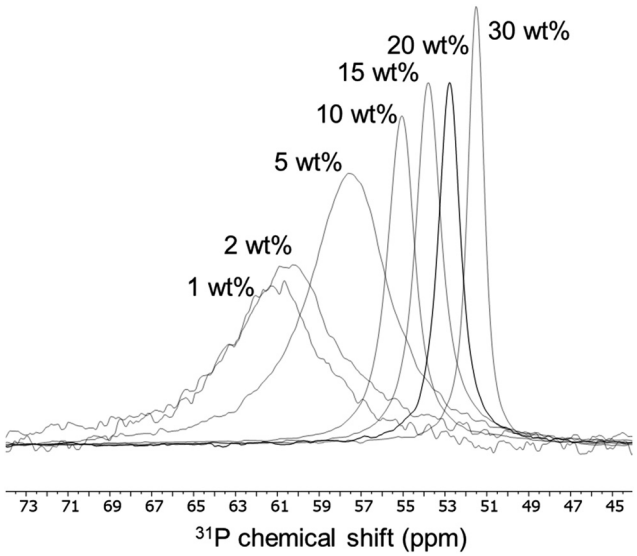

Fig. 2 Variation of ^{31}P chemical shift and linewidth of adsorbed TEPO at different loadings on Aerosil 200 calcined at 500 °C.

the isolated species. The decrease in temperature produced an enlargement of the signal, in agreement with a slower exchange, but also the appearance of spinning side bands, due to a hindered rotation of the TEPO molecules (Fig. S3, ESI†). However, the interference of cooling and spinning made impossible the MAS at 10 kHz below 200 K, giving rise to intense and close spinning side bands that precluded the detection of the isolated species.

Taking into account the BET surface area of Aerosil (200 m^2 g^{-1}) and considering an evenly distribution of TEPO on the surface, the TEPO coverage should vary from 0.22 to 6.73 molecules per nm^2. When the ^{31}P δ is represented against the surface coverage, two distinct zones can be observed (Fig. 3). At high coverage, the chemical shift varies smoothly with a low slope, whereas at low coverage the variation has a much higher slope. This behaviour is analogous to that observed in solution with Brønsted acids (Fig. S4, ESI†).

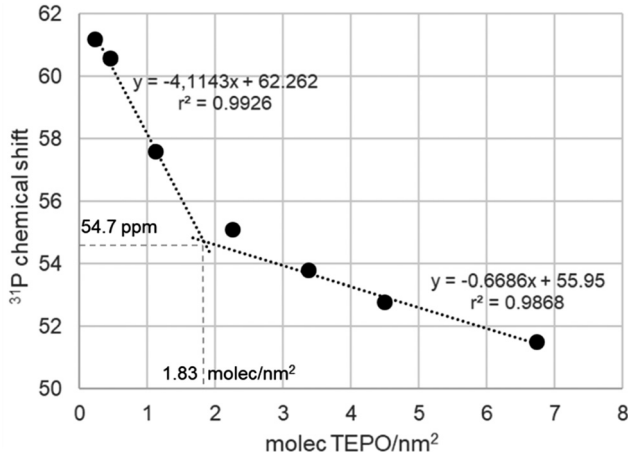

Fig. 3 Variation of ^{31}P chemical shift (ppm) of adsorbed TEPO at different surface coverages on Aerosil 200 calcined at 500 °C.

Both straight lines cross at a coverage of 1.83 molecules per nm^2. Interestingly, the Zhuravlev model[16] describes a silanol density of 1.80 OH nm^{-2} at 500 °C, the same value obtained in Fig. 3 for the change of tendency of the ^{31}P δ of adsorbed TEPO. This seems to indicate that the cross point corresponds to the 1:1 silanol/TEPO molar ratio and hence the value of 54.7 ppm could be considered as the $\delta_{1:1}$ value for the SiO–H···O═PEt$_3$, in good agreement with the values for different silanol species determined in solution (in the range of 51.5–53.4 for isolated silanols).[23] Moreover, according to our correlation in solution,[13] the pK_a of silanols should be 11.5, similar to TFE and not too far from the value determined in solution for triethylsilanol (13.6),[24] taking into account the structural differences and the completely different conditions used for the measurements. This result contrasts with much stronger acidity values reported in the literature (from both theoretical and experimental studies) for silanol groups on silica.[25–28]

At TEPO loadings below 1.83, the important variation of the chemical shift seems to indicate the existence of a second species on the surface, due to the excess of acid sites over TEPO, in a similar way to the observation in solution that was assigned to the 2:1 acid–TEPO species. In the case of silica, this species must be the (Si–OH)$_2$···O═PEt$_3$, whose chemical shift can be estimated as 62.3 ppm extrapolating at zero coverage. This value would be comparable with the ^{31}P chemical shift of TEPO at infinite dilution in liquid phase (method for determination of AN of solvents[4]), slightly higher than in methanol (60.3 ppm) and lower than in acetic acid (65.2 ppm) or trifluoroethanol (65.6 ppm).

Species with two hydrogen bonds to TEPO has been detected in the X-ray crystal structure of a complex with bis-dihydrotetrazine (H$_4$btzp^{Me}) as double hydrogen bond donor.[29] The distance between the two donor N atoms in H$_4$btzp^{Me} is 4.8 Å (Fig. 4), whereas in models for amorphous silica surface,[30] neighbour isolated silanols (with only a siloxane between them) show a distance of 4.6 Å between the two oxygen atoms (Fig. 4), being then compatible with the formation of the proposed (Si–OH)$_2$···O═P species.

According to the Zhuravlev model,[16] the calcination of a silica at 200 °C should leave a fully hydroxylated surface with a silanol density of 4.6 OH nm^{-2}. Thus, the dependence of the

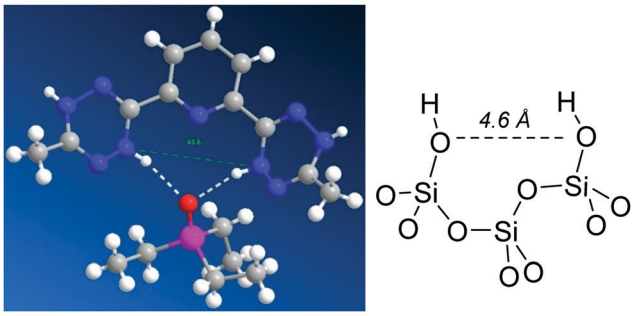

Fig. 4 Measurement of the N–N distance in the H$_4$btzp^{Me}·OPEt$_3$ complex[29] and comparison with the O–O distance between two neighbour isolated silanols in a model[30] of amorphous silica surface.

Open Access Article. Published on 27 June 2022. Downloaded on 10/30/2025 7:29:39 PM.
This article is licensed under a Creative Commons Attribution-NonCommercial 3.0 Unported Licence.

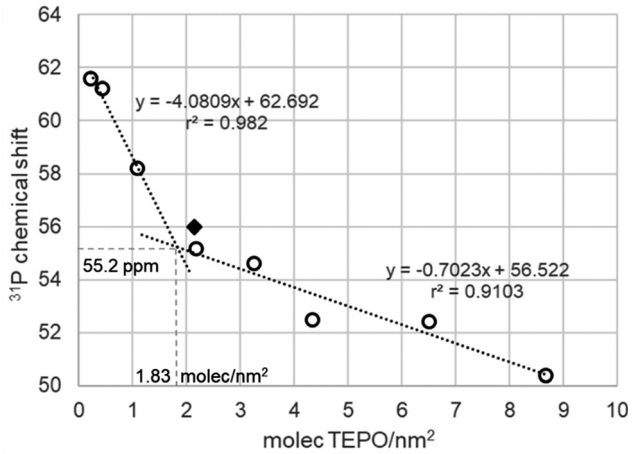

Fig. 5 Variation of ^{31}P chemical shift (ppm) of adsorbed TEPO at different surface coverages on Aerosil 200 calcined at 200 °C. Diamond: result described for silica gel in ref. 5.

chemical shift with the coverage of adsorbed TEPO on Aerosil 200 calcined at 200 °C should be significantly different from that of the same silica calcined at 500 °C. On the contrary, the spectra of TEPO adsorbed with loadings in the range of 1–40 wt% show an analogous trend (Fig. 5) as in the absorption on Aerosil calcined at 500 °C and with nearly the same linewidth. In the same figure it has been represented one result reported in the literature,[5] showing an excellent agreement with our own measurements.

The calculation of the apparent silanol density using the cross point leads to a value of 1.83 molecules per nm^2, far from the expected value of 4.6 molecules per nm^2 according to the Zhuravlev model. However, if the distribution of the different types of silanols is taken into account, at 200 °C it includes 1.2 OH nm^{-2} isolated, 0.6 OH nm^{-2} geminal, and 2.8 OH nm^{-2} vicinal silanols, and the apparent silanol density from TEPO adsorption agrees with the (geminal + isolated) density (1.8 OH nm^{-2}). Vicinal silanols are linked by hydrogen bonds. The H-bond donor silanol may not react with TEPO, as it happens with diols and weakly H-bond acceptors,[31] but in principle a H-bond acceptor silanol should be even more acidic than an isolated one.[32] However, it has been described that silanols can be placed in highly dense zones, called nests. In the case of zeolites, triads[33] and tetrads[34] have been described, in which all the silanols are at the same time H-bond donors and acceptors. In fact, it has been argued that silanols arranged in this type of structure do not participate in the polarity of the surface,[34] in agreement with our observation in the case of silica. This kind of regular structures is very unlikely in the case of amorphous silica, but H-bond donation to siloxane bonds[35] can also be considered for the lack of free silanols in nests.

One method to open the silanol hydrogen bond network would be the use of a protic solvent such as methanol for TEPO adsorption. In this way, TEPO should be able to interact with a larger amount of silanols in competence with the remaining methanol molecules. In fact, the chemical shifts obtained after adsorption from methanol solution showed a significant variation, but the values were not fully reproducible. The lack of reproducibility must be ascribed to the difficulty in controlling the amount of remaining methanol after evaporation that influences the results. This hypothesis seems to be confirmed by the fact that a thorough evaporation and total elimination of methanol leads to the same chemical shift values as the ones obtained from hexane solution.

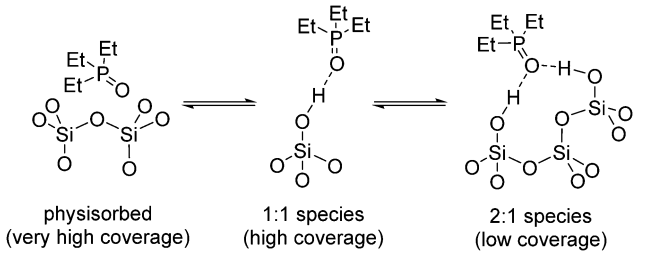

Scheme 1 Proposed equilibria of adsorbed TEPO species on the silica surface.

As pointed above, the presence of a single ^{31}P NMR points to a rather fast equilibrium between different surface species (Scheme 1). At high TEPO loading, the equilibrium would be stablished between physisorbed TEPO and 1:1 silanol–TEPO species. At low TEPO loading, the equilibrium present on the surface would be between 1:1 silanol–TEPO and 2:1 (silanol)$_2$–TEPO species. The broadening of the signal at low TEPO loading is also in agreement with the equilibrium hypothesis. Whereas in the studies in solution the exchange rate is usually controlled by the temperature,[36] on a surface the exchange rate should be controlled by the distance between the species to be exchanged, which will be longer as the surface density decreases (low surface coverage). This is fully confirmed by the dependence (Fig. 6) of linewidth (Full Width at Half Maximum, FWHM) with surface coverage (σ), showing that FWHM $\sim 1/\sqrt{\sigma}$, that is the average nearest-neighbour distance between TEPO molecules on the surface.[37] The rather high dispersion of results at low coverage may be due to the presence of residual hexane, which might increase the mobility on the

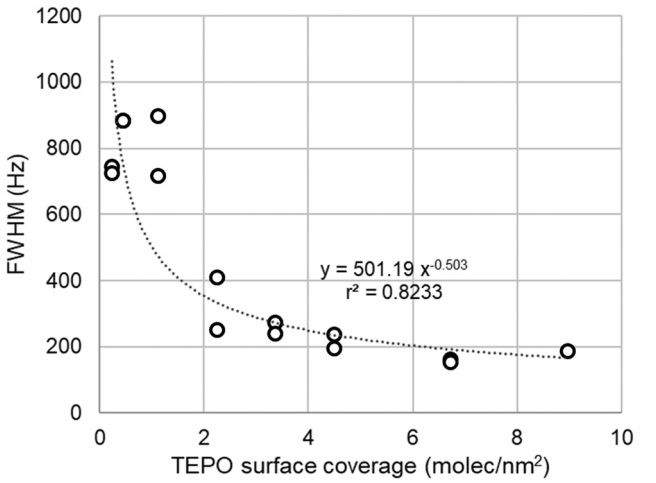

Fig. 6 Dependence of the linewidth of TEPO ^{31}P signal with the surface coverage in the case of Aerosil 200.

Open Access Article. Published on 27 June 2022. Downloaded on 10/30/2025 7:29:39 PM.
This article is licensed under a Creative Commons Attribution-NonCommercial 3.0 Unported Licence.

surface, speeding up the exchange process in a uncontrolled manner, this effect being more evident at low TEPO loadings.[38]

TEPO adsorption on MCM-41

If the Zhuravlev model is correct and the surface silanol density is constant at the same temperature for all the types of silicas, the values of ^{31}P chemical shifts for adsorbed TEPO should be the same as on Aerosil at the same surface coverage, irrespective of the surface area. The surface area of MCM-41 is much larger (near 1000 m^2 g^{-1}) than that of Aerosil 200. Furthermore, it is a crystalline mesoporous solid, allowing then the study of the effect of porosity on the distribution of TEPO. The δ values for TEPO loadings between 5 and 40 wt% are shown in Fig. 7. As it corresponds to its much larger surface area, the loading range is fully included in the high slope part of the graph (low coverage) and the values fit perfectly with the line obtained with Aerosil (Fig. 7, grey lines). This result confirms the Zhuravlev model about the similar nature of the silica surface irrespective from its nature and textural properties. The nearly identical values obtained on MCM-41 calcined at 500 and 200 °C (Fig. 7) show again the lack of interaction of TEPO with the vicinal silanols linked with hydrogen bonds, and the detection of only the isolated and geminal ones.

TEPO adsorption on Silia P60

As it was interesting to check a porous non-regular material to check the effect of this non-periodic structure, a similar study was performed with Silia P60. Silia P60 is an amorphous precipitated silica, with irregular surface and porosity. The surface area is around 450 m^2 g^{-1}, that is, an intermediate value between Aerosil 200 and MCM-41. The pore volume is similar to that of MCM-41, but the pores are not regular and the pore size distribution is much wider (Fig. S1, ESI†). These properties might interfere in the TEPO diffusion and distribution and it would be interesting to check this point. According

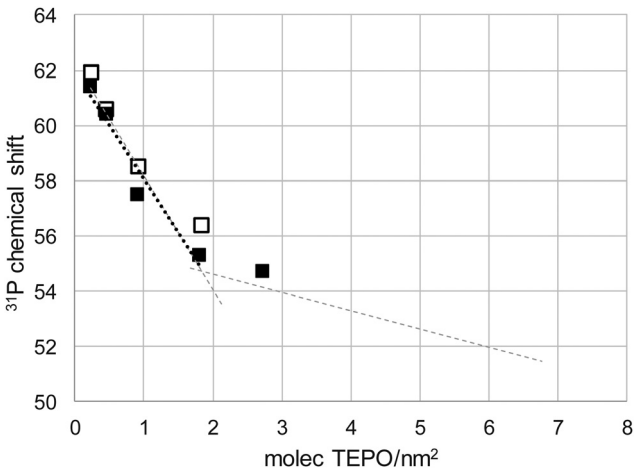

Fig. 7 Variation of ^{31}P chemical shift (ppm) of adsorbed TEPO at different surface coverages on MCM-41 calcined at 500 °C (filled squares and dotted line) and 200 °C (open squares). The tendency lines for TEPO adsorbed on Aerosil calcined at 500 °C are included in grey for the sake of comparison.

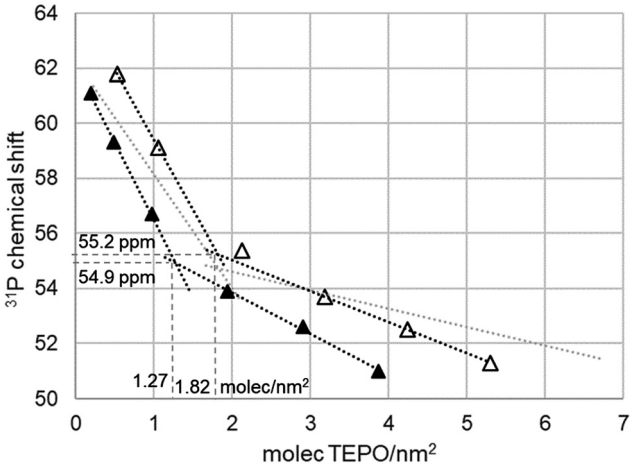

Fig. 8 Variation of ^{31}P chemical shift (ppm) of adsorbed TEPO at different surface coverages on Silia P60 calcined at 500 °C (filled symbols) and 200 °C (open symbols). The tendency lines for TEPO adsorbed on Aerosil calcined at 500 °C are included in grey for the sake of comparison.

to the previous results and the Zhuravlev model, the dependence of ^{31}P δ with the surface coverage should be the same as on Aerosil. However, this is not the case, as can be seen in Fig. 8. In the case of Silia P60 calcined at 500 °C, the values are lower than expected, whereas for Silia P60 calcined at 200 °C they are higher at low coverage. In both cases the tendency lines show a higher slope than in the case of Aerosil, and they are nearly parallel for both calcination temperatures, showing the consistency of the measurements. As a result, the cross point in Silia P60 calcined at 200 °C appears at nearly the same $\delta_{1:1}$, 55.2 ppm, and surface coverage, 1.82 molecules per nm^2, as in the case of Aerosil (54.7 ppm and 1.83 molecules per nm^2). However, the result is much different for Silia P60 calcined at 500 °C with respect to surface coverage, only 1.27 molecules per nm^2, although the $\delta_{1:1}$ remains constant (54.9 ppm).

This result can be interpreted as a lack of accessibility of TEPO to part of the silica surface, due to the tortuosity of the irregular pore system. As the detected silanol density is 70% of that determined in the Zhuravlev model, it can be considered that only 70% of the surface is accessible (only 328 of the total 463 m^2 g^{-1}). However, the higher slopes and the higher values of chemical shift at low coverage in Silia P60 calcined at 200 °C seem to indicate a distribution of the silanol types on the surface different from that on Aerosil or MCM-41. In fact, the values of the Zhuravlev model are averages, and the values for each type of silica show a certain variability. For example, the silanol density on silicas calcined at 500 °C has shown to be in the range of 1.45–2 OH nm^{-2}.[16] Hence, the variation in TEPO ^{31}P δ can be ascribed to this variability.

In spite of this deviation of Silia P60 from the behavior of the most regular silicas (Aerosil and MCM-41), the relationship of the linewidth and the surface coverage remains stable within all the solids tested (Fig. 9). Although with a slightly higher dispersion of data, the adjust is similar and confirms the dependence with $1/\sqrt{\sigma}$, that is the average nearest-neighbour

Open Access Article. Published on 27 June 2022. Downloaded on 10/30/2025 7:29:39 PM.
This article is licensed under a Creative Commons Attribution-NonCommercial 3.0 Unported Licence.

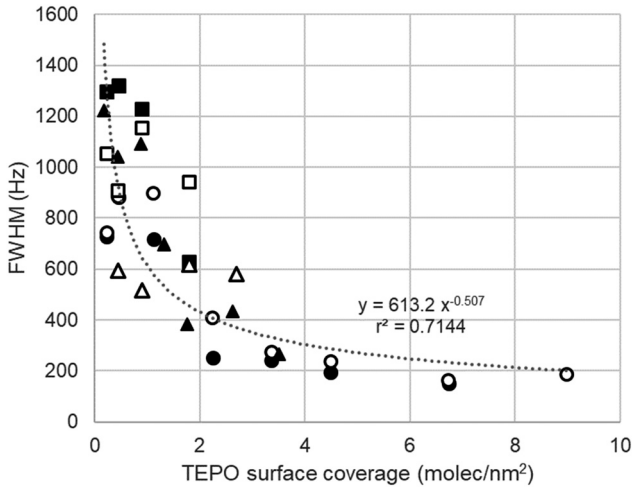

Fig. 9 Dependence of the linewidth of TEPO ^{31}P signal with the surface coverage in silicas pretreated at 200 °C (open symbols) and 500 °C (filled symbols): Aerosil 200 (●), MCM-41 (■), and Silia P60 (▲).

distance between TEPO molecules on the surface.[37] The longest distance will imply a slower exchange and hence a wider signal.

Conclusions

The adsorption of different amounts TEPO on silica produces a significant variation in the ^{31}P chemical shift of a single NMR signal. This observation demonstrates the existence of a rather fast equilibrium between different adsorbed species. Moreover, the dependence of the chemical shift with surface coverage with TEPO shows two types of equilibria, between physisorbed TEPO and silanol–TEPO 1 : 1 species at high coverage, and between silanol–TEPO 1 : 1 and 2 : 1 species at low coverage. The 2 : 1 species must come from neighbour silanols, but far enough to be isolated, given that the vicinal silanols are not detectable for TEPO, which is not able to break the hydrogen bond between them. As a general conclusion, the acid strength of a solid, at least in a weak acidic solid such as silica, cannot be determined by a single NMR measurement of adsorbed TEPO and several measurements at different surface coverage are required for a complete picture of the nature of the surface acid sites. This behaviour should be general for all the phosphine oxides, such as TMPO or TBPO, and all the silica-based solids, unless microporosity can limit the access and diffusion to part of the silica surface. The possibility of exchange between stronger acid sites and between strong and weak sites is currently under study.

Conflicts of interest

There are no conflicts to declare.

Acknowledgements

This work was financially supported by the Spanish Ministerio de Ciencia, Innovación y Universidades (project number RTI2018-093431-B-I00), the Gobierno de Aragón (E37_20R group) and co-financed with Feder 2014–2020 "Construyendo Europa desde Aragón".

Notes and references

1 A. Zheng, S.-J. Huang, S.-B. Liu and F. Deng, *Phys. Chem. Chem. Phys.*, 2011, **13**, 14889–14901.
2 A. Zheng, S. Bin Liu and F. Deng, *Chem. Rev.*, 2017, **117**, 12475–12531.
3 J. P. Osegovic and R. S. Drago, *J. Catal.*, 1999, **182**, 1–4.
4 V. Gutmann, *Coord. Chem. Rev.*, 1976, **18**, 225–255.
5 J. P. Osegovic and R. S. Drago, *J. Phys. Chem. B*, 2000, **104**, 147–154.
6 A. Zheng, S. J. Huang, W. H. Chen, P. H. Wu, H. Zhang, H. K. Lee, L. C. De Ménorval, F. Deng and S. Bin Liu, *J. Phys. Chem. A*, 2008, **112**, 7349–7356.
7 A. Zheng, H. Zhang, X. Lu, S. Bin Liu and F. Deng, *J. Phys. Chem. B*, 2008, **112**, 4496–4505.
8 D. Margolese, J. A. Melero, S. C. Christiansen, B. F. Chmelka and G. D. Stucky, *Chem. Mater.*, 2000, **12**, 2448–2459.
9 P. A. Russo, M. M. Antunes, P. Neves, P. V. Wiper, E. Fazio, F. Neri, F. Barreca, L. Mafra, M. Pillinger, N. Pinna and A. A. Valente, *J. Mater. Chem. A*, 2014, **2**, 11813–11824.
10 C. Bispo, K. De Oliveira Vigier, M. Sardo, N. Bion, L. Mafra, P. Ferreira and F. Jérôme, *Catal. Sci. Technol.*, 2014, **4**, 2235–2240.
11 M. M. Antunes, P. A. Russo, P. V. Wiper, J. M. Veiga, M. Pillinger, L. Mafra, D. V. Evtuguin, N. Pinna and A. A. Valente, *ChemSusChem*, 2014, **7**, 804–812.
12 B. Garg, T. Bisht and Y.-C. Ling, *RSC Adv.*, 2014, **4**, 57297–57307.
13 E. Pires and J. M. Fraile, *Phys. Chem. Chem. Phys.*, 2020, **22**, 24351–24358.
14 P. Fernández, M. J. Fraile, E. García-Bordejé and E. Pires, *Catalysts*, 2019, **9**, 804.
15 J. M. Fraile, E. García-Bordejé, E. Pires and L. Roldán, *J. Catal.*, 2015, **324**, 107–118.
16 L. T. Zhuravlev, *Colloids Surf., A*, 2000, **173**, 1–38.
17 V. Y. Davydov, A. V. Kiselev and L. T. Zhuravlev, *Trans. Faraday Soc.*, 1964, **60**, 2254–2264.
18 A. Burneau, O. Barres, J. Gallas and J. C. Lavalley, *Langmuir*, 1990, **6**, 1364–1372.
19 B. A. Morrow and A. J. McFarlan, *J. Phys. Chem.*, 1992, **96**, 1395–1400.
20 C. C. Liu and G. E. Maciel, *J. Am. Chem. Soc.*, 1996, **118**, 5103–5119.
21 S. Ek, A. Root, M. Peussa and L. Niinistö, *Thermochim. Acta*, 2001, **379**, 201–212.
22 X. Yi, H. H. Ko, F. Deng, S. Bin Liu and A. Zheng, *Nat. Protoc.*, 2020, **15**, 3527–3555.
23 K. M. Diemoz and A. K. Franz, *J. Org. Chem.*, 2019, **84**, 1126–1138.
24 P. D. Lickiss, *Adv. Inorg. Chem.*, 1995, **42**, 147–262.

 This journal is © the Owner Societies 2022

Open Access Article. Published on 27 June 2022. Downloaded on 10/30/2025 7:29:39 PM.
This article is licensed under a Creative Commons Attribution-NonCommercial 3.0 Unported Licence.

25 S. Ong, X. Zhao and K. B. Eisenthal, *Chem. Phys. Lett.*, 1992, **191**, 327–335.
26 Y. Duval, J. A. Mielczarski, O. S. Pokrovsky, E. Mielczarski and J. J. Ehrhardt, *J. Phys. Chem. B*, 2002, **106**, 2937–2945.
27 M. Sulpizi, M. P. Gaigeot and M. Sprik, *J. Chem. Theory Comput.*, 2012, **8**, 1037–1047.
28 X. Liu, J. Cheng, X. Lu and R. Wang, *Phys. Chem. Chem. Phys.*, 2014, **16**, 26909–26916.
29 A. V. Polezhaev, N. A. Maciulis, C. H. Chen, M. Pink, R. L. Lord and K. G. Caulton, *Chem. – Eur. J.*, 2016, **22**, 13985–13998.
30 A. Comas-Vives, *Phys. Chem. Chem. Phys.*, 2016, **18**, 7475–7482.
31 L. Weirich, J. Magalhães De Oliveira and C. Merten, *Phys. Chem. Chem. Phys.*, 2020, **22**, 1525–1533.
32 L. R. Snyder and J. W. Ward, *J. Phys. Chem.*, 1966, **70**, 3941–3952.
33 C. Schroeder, C. Mück-Lichtenfeld, L. Xu, N. A. Grosso-Giordano, A. Okrut, C. Y. Chen, S. I. Zones, A. Katz, M. R. Hansen and H. Koller, *Angew. Chem., Int. Ed.*, 2020, **59**, 10939–10943.
34 T. Kawai and K. Tsutsumi, *J. Colloid Interface Sci.*, 1999, **212**, 310–316.
35 K. Nassau and K. Raghavachari, *J. Non-Cryst. Solids*, 1988, **104**, 181–189.
36 A. D. Bain, *Prog. Nucl. Magn. Reson. Spectrosc.*, 2003, **43**, 63–103.
37 P. P. Bansal and A. J. Ardell, *Metallography*, 1972, **5**, 97–111.
38 R. L. Johnson, M. P. Hanrahan, M. Mellmer, J. A. Dumesic, A. J. Rossini and B. H. Shanks, *J. Phys. Chem. C*, 2017, **121**, 17226–17234.